Bioorganic & Medicinal Chemistry 26 (2018) 5742–5750

Contents lists available at ScienceDirect

Bioorganic & Medicinal Chemistry

journal homepage: www.elsevier.com/locate/bmc

Synthetic thiosemicarbazones as a new class of *Mycobacterium tuberculosis* protein tyrosine phosphatase A inhibitors

Larissa Sens[a], Ana Caroline Arruda de Souza[b], Lucas Antonio Pacheco[a], Angela Camila Orbem Menegatti[b,*], Mattia Mori[c], Alessandra Mascarello[a], Ricardo José Nunes[a], Hernán Terenzi[b,*]

[a] *Laboratório Estrutura e Atividade, Departamento de Química, LEAT-CFM-UFSC, Universidade Federal de Santa Catarina, Campus Trindade, 88040-900 Florianópolis, SC, Brazil*

[b] *Centro de Biologia Molecular Estrutural, Departamento de Bioquímica, CEBIME-UFSC, Universidade Federal de Santa Catarina, Campus Trindade, 88040-900 Florianópolis, SC, Brazil*

[c] *Department of Biotechnology, Chemistry and Pharmacy, University of Siena. Via Aldo Moro 2, 53100 Siena, Italy*

ARTICLE INFO

Keywords:
Tuberculosis
PtpA
Inhibitors
Thiosemicarbazones

ABSTRACT

Mycobacterium tuberculosis secretes two protein tyrosine phosphatases as virulence factors, PtpA and PtpB. Inhibition studies of these enzymes have shown significant attenuation of the *M. tuberculosis* growth *in vivo*. As PtpA mediates many effects on the regulation of host signaling ensuring the intracellular survival of the bacterium we report, for the first time, thiosemicarbazones as potential novel class of PtpA inhibitors. Several compounds were synthesized and biologically evaluated, revealing interesting results. Enzyme kinetic assays showed that compounds **5**, **9** and **18** are non-competitive inhibitors of PtpA, with K_i values ranging from 1.2 to 5.6 μM. Modeling studies clarified the structure-activity relationships observed *in vitro* and indicated a possible allosteric binding site in PtpA structure. To the best of our knowledge, this is the first disclosure of potent non-competitive inhibitors of PtpA with great potential for future studies and development of analogues.

1. Introduction

Mycobacterium tuberculosis (*Mtb*) causes tuberculosis (TB), an infectious-contagious disease that is one of the top 10 causes of death worldwide. In 2017, 1.3 million people died from TB and 10 million became ill.[1] For many years, the same first-line anti-TB drugs have been used to combat the disease, but there are numerous reports of strains resistant to this treatment. An alternative is to use a second-line of antibiotics, which has disadvantages, such as major side-effects, long duration, and high costs. In addition, cases of strains resistant to second-line anti-TB drugs have already been reported.[1–3]

As a result, the scientific community has turned its attention to the research of new TB treatments with different mechanisms of action from those already in use. *Mtb* resides within macrophages, which are the cells responsible for the activation of the immune response necessary to control and eliminate the invasion of microorganisms.[4,5] *Mtb* has developed a strategy to remain alive within macrophages, secreting several immunogenic proteins that modulate the immune response of the host, among which are protein kinases and phosphatases, such as protein tyrosine phosphatases (PTPs).[6–9]

Two tyrosine phosphatases, PtpA and PtpB, were shown to be involved in the survival of the bacterium[10–12] and that their inhibition attenuates the growth of *Mtb* and the infection in animal models, thus becoming targets for the development of new anti-TB drugs.[8,13–20]

Our research group has been focusing efforts on the development of new, more potent and selective inhibitors of PtpA and PtpB. Several chalcones have been studied by our group; some naphthyl chalcones were found to be excellent inhibitors of PtpA or PtpB[15,21,22] and some sulfonyl hydrazones excellent competitive inhibitors of PtpB.[23]

From this came the interest in studying a novel class of compounds as PtpA inhibitors. Thiosemicarbazones constitute an important class of compounds whose properties have been extensively studied in Medicinal Chemistry,[24] displaying a wide range of biological activities, such as antifungal,[25] antitumor,[26,27] antiviral,[28,29] antimicrobial,[30,31] and antibacterial properties.[32]

This class of compounds has been shown to comprise good enzyme inhibitors, acting, for example, on the enzyme tyrosinase, which is involved in the development of melanomas,[33] and on cysteine proteases, which are essential for several functions of the malaria parasite.[34] Moreover, the thiosemicarbazone triapine, a very potent inhibitor of

* Corresponding authors.
E-mail addresses: angelamenegatti@yahoo.com.br (A.C.O. Menegatti), hernan.terenzi@ufsc.br (H. Terenzi).

https://doi.org/10.1016/j.bmc.2018.10.030
Received 20 July 2018; Received in revised form 1 October 2018; Accepted 26 October 2018
Available online 27 October 2018

Table 1
Synthesis of thiosemicarbazones **4–52**.

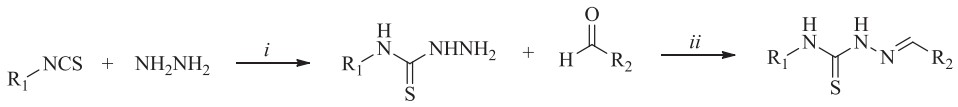

1, R= 1-naphthyl
2, R= 4-CH_3-Ph
3, R= 4-OCH_3-Ph

Compound	R_1	R_2	Compound	R_1	R_2
4	1-naphthyl	Ph	**29**	4-CH_3-Ph	1-naphthyl
5	1-naphthyl	4-NO_2-Ph	**30**	4-CH_3-Ph	2-naphthyl
6	1-naphthyl	4-Cl-Ph	**31**	4-CH_3-Ph	3,4-diCl-Ph
7	1-naphthyl	4-OCH_3-Ph	**32**	4-CH_3-Ph	2,5-diOCH_3-Ph
8	1-naphthyl	3,4-OCH_2O-Ph	**33**	4-CH_3-Ph	3,4-diOCH_3-Ph
9	1-naphthyl	4-Ph-Ph	**34**	4-CH_3-Ph	2-NO_2-Ph
10	1-naphthyl	3-OCH_3,4-OH-Ph	**35**	4-CH_3-Ph	5-(2-Cl,5-CF_3)-Ph-furan-2-yl
11	1-naphthyl	3,4,5-triOCH_3-Ph	**36**	4-CH_3-Ph	4-N(CH_3)-Ph
12	1-naphthyl	1-naphthyl	**37**	4-OCH_3-Ph	Ph
13	1-naphthyl	2-naphthyl	**38**	4-OCH_3-Ph	4-CH_3-Ph
14	1-naphthyl	3,4-diCl-Ph	**39**	4-OCH_3-Ph	4-NO_2-Ph
15	1-naphthyl	2,5-diOCH_3-Ph	**40**	4-OCH_3-Ph	4-Cl-Ph
16	1-naphthyl	3,4-diOCH_3-Ph	**41**	4-OCH_3-Ph	4-OCH_3-Ph
17	1-naphthyl	2-NO_2-Ph	**42**	4-OCH_3-Ph	3,4-OCH_2O-Ph
18	1-naphthyl	5-(2-Cl,5-CF_3)-Ph-furan-2-yl	**43**	4-OCH_3-Ph	4-Ph-Ph
19	1-naphthyl	4-N(CH_3)-Ph	**44**	4-OCH_3-Ph	3-OCH_3,4-OH-Ph
20	4-CH_3-Ph	Ph	**45**	4-OCH_3-Ph	3,4,5-triOCH_3-Ph
21	4-CH_3-Ph	4-CH_3-Ph	**46**	4-OCH_3-Ph	1-naphthyl
22	4-CH_3-Ph	4-NO_2-Ph	**47**	4-OCH_3-Ph	2-naphthyl
23	4-CH_3-Ph	4-Cl-Ph	**48**	4-OCH_3-Ph	3,4-diCl-Ph
24	4-CH_3-Ph	4-OCH_3-Ph	**49**	4-OCH_3-Ph	2,5-diOCH_3-Ph
25	4-CH_3-Ph	3,4-OCH_2O-Ph	**50**	4-OCH_3-Ph	3,4-diOCH_3-Ph
26	4-CH_3-Ph	4-Ph-Ph	**51**	4-OCH_3-Ph	2-NO_2-Ph
27	4-CH_3-Ph	3-OCH_3,4-OH-Ph	**52**	4-OCH_3-Ph	4-N(CH_3)-Ph
28	4-CH_3-Ph	3,4,5-triOCH_3-Ph			

(*i*) Isopropanol, r.t.; (*ii*) ethanol/water, acetic acid, reflux; Ph = phenyl.

ribonucleotide reductase (RNR), is a promising molecule for anticancer therapy.[35] In more recent studies, iminodiacetate-thiosemicarbazones and their dicopper(II) complexes have also been found to be RNR inhibitors.[36]

Based on these observations, the aim of this study was to synthesize thiosemicarbazones as potential PtpA inhibitors that could be used in TB therapy. The compounds were assayed to investigate their PtpA inhibitory activity, potency, and selectivity. In addition, we investigated the inhibition mechanism involved, using the four most potent thiosemicarbazone in enzyme kinetic assays. To provide new insights into the mechanism of inhibition and binding of PtpA inhibitors we performed molecular docking simulations.

2. Results and discussion

A chemical library of 49 thiosemicarbazones (**4–52**) was produced in two stages, according to the scheme on Table 1. First, the synthesis of thiosemicarbazides **1–3** was performed by the reaction between different isothiocyanates and hydrazine hydrate in isopropanol.[37] The thiosemicarbazides were used in subsequent reactions with different aldehydes, using acetic acid as a catalyst in a solvent mixture of water/ethanol.[30] The synthesized compounds presented yields in the range of 60–90%, were characterized by melting point (mp), ^{1}H and ^{13}C nuclear magnetic resonance (NMR) spectroscopy, and had their structures confirmed by high-resolution mass spectrometry (HRMS). Thiosemicarbazones **6**, **8**, **9**, **11–18**, **44**, **45**, **47**, **48**, **50**, and **51** have not been reported in the literature.

The spectral characterization of the compounds (**4–19** and **37–52**) is detailed in the Experimental and Supplementary Information Sections. ^{1}H NMR spectra revealed that all structures had an *E* configuration, with the N—H chemical shifts appearing as two singlets at around 10–11 ppm[38] and the iminic hydrogen as a singlet at 7–8 ppm. The synthesis of thiosemicarbazones **20–36** was previously reported by the authors.[39]

Table 2
Percentage of PtpA inhibition at the single concentration of 25 μM and IC_{50} of the most active compounds[a].

Compd	PtpA inhibition (%)	IC_{50} (μM)	Compd	PtpA inhibition (%)	IC_{50} (μM)
4	58.1 ± 5.3	nd	**29**	33.7 ± 1.0	nd
5	77.7 ± 5.1	9.5 ± 3.3	**30**	29.3 ± 1.2	nd
6	0	nd	**31**	23.4 ± 4.2	nd
7	22.6 ± 3.9	nd	**32**	2.8 ± 2.2	nd
8	62.6 ± 3.0	17.8 ± 0.6	**33**	6.6 ± 1.8	nd
9	79.7 ± 1.8	7.4 ± 2.8	**34**	21.6 ± 2.0	nd
10	0	nd	**35**	66.0 ± 0.6	9.1 ± 5.0
11	0	nd	**36**	35.4 ± 3.4	nd
12	10.3 ± 1.6	nd	**37**	0	nd
13	67.7 ± 5.2	23.7 ± 2.9	**38**	0	nd
14	83.7 ± 3.5	13.4 ± 2.2	**39**	64.4 ± 3.5	15.1 ± 5.8
15	44.2 ± 2.1	nd	**40**	1.0 ± 9.3	nd
16	64.5 ± 4.6	18.2 ± 2.2	**41**	0	nd
17	52.4 ± 2.0	nd	**42**	0	nd
18	86.7 ± 0.8	2.9 ± 1.7	**43**	41.2 ± 8.4	nd
19	51.6 ± 1.2	nd	**44**	6.6 ± 1.8	nd
20	16.6 ± 2.3	nd	**45**	0	nd
21	0.7 ± 7.5	nd	**46**	22.7 ± 1.8	nd
22	37.2 ± 1.8	nd	**47**	23.7 ± 7.0	nd
23	4.9 ± 5.6	nd	**48**	21.4 ± 3.7	nd
24	8.9 ± 2.9	nd	**49**	0	nd
25	25.9 ± 1.5	nd	**50**	0	nd
26	26.3 ± 3.3	nd	**51**	0	nd
27	8.8 ± 1.6	nd	**52**	3.9 ± 4.0	nd
28	0	nd			

[a] Data are expressed as means ± SD of three independent experiments. Compd = compound; nd = not determined.

The inhibitory activity of the thiosemicarbazone derivatives was evaluated *in vitro* against recombinant PtpA from *Mtb*, using *p*-nitrophenyl phosphate (*p*NPP) as substrate. The percentage of inhibition was assessed spectrophotometrically at a single concentration (25 μM) for each compound of the series. As shown in Table 2, several compounds were active against the enzyme, with the percentage of inhibition reaching 87%. Specifically, the results indicate that 22 out of 50 compounds (**4–6**, **8**, **9**, **13–19**, **22**, **25**, **26**, **29**, **30**, **35**, **36**, **39**, and **43**) exhibited inhibitory activity against PtpA (inhibition > 25%).

Among these 22 active compounds, only those that reached inhibition results higher than 60% (**5**, **8**, **9**, **13**, **14**, **16**, **18**, **35**, and **39**) were selected for IC_{50} assays, which were performed to better understand the potency involved in the inhibition of PtpA (Table 2). The compounds showed substantial PtpA inhibition, with IC_{50} values lower than 24 μM (Table 2).

The series that presented a higher number of active compounds had a 1-naphthyl substituent in R_1, thus this group seems to be important for thiosemicarbazones activity against PtpA. This was an interesting result, in a previous study by our research group, it was observed that hydrophobic groups appear to be promising for the inhibition of PtpA by chalcone derivatives, a chemical class different from that presented in this work.[21] For chalcones, this effect was explained by the presence of π−π interactions between the 2-naphthyl substituent (at ring B) of competitive inhibitors and the side chain residue Trp48 of the PtpA binding site.[15]

By comparing the three different R_1 substituents (1-naphthyl, 4-CH_3-Ph, and 4-OCH_3-Ph), we noted that when the electron-donor effect of the substituent increases the inhibitory activity tends to decrease. Regarding the R_2 substituents of the compounds with marked PtpA inhibition, electron-withdrawing groups tend to enhance the inhibitory activity. This effect was most evident for compounds **5**, **9**, **14**, **18**, **35**, and **39**.

In addition, it is interesting to note the results found for compounds **12** and **13**, both having 1-naphthyl substituent at R_1, but in R_2 the groups are 1-naphthyl and 2-naphthyl, respectively. Compound **12** showed 10% inhibition of PtpA activity while the thiosemicarbazone **13** showed an inhibition of 68%. In previous studies of our group it was reported that a chalcone derived from 2-naphthyl was five times more potent than the same derivative of 1-naphthyl, due to the 2-naphthyl positioning which favored the pi-stacking interaction.[15,21] Observing compounds **30** and **47**, which also have a 2-naphthyl at R_2, we did not observe significant inhibition of PtpA activity, at most 30% inhibition, this finding indicates that for the thiosemicarbazones studied the 1-naphthyl in R_1 is extremely important for the inhibitory activity.

The best PtpA inhibition result was achieved with compound **18** (IC_{50} = 2.9 ± 1.7 μM), derived from 1-naphthyl and 5-(2-Cl,5-CF_3)-Ph-furan-2-yl. A study has previously reported that benzanilide derivatives with electron-withdrawing groups at the *meta* and *para* positions result in a substantial improvement in PtpA inhibition, and that the presence of a trifluoromethyl group (CF_3) leads to higher binding affinity, which is explained by the pi-stacking with Trp48 of the enzyme's active site.[40] In addition, the most potent and selective PtpA inhibitor described in the literature[19] presents a scaffold similar to that described by Rawls[40], with electron-withdrawing groups in its structure. Compound **18** resembles these inhibitors by the presence of electron withdrawing groups, but our work differs in that it has an apolar group that is important for inhibition of PtpA. In that work, the most active compounds presented hydrophobic groups in R_1 and polar substituents in R_2.

Selectivity is a great challenge in the development of PTP inhibitors since the active site is highly conserved across the family and most PTPs of pharmaceutical interest have close human homologs, which would cause adverse effects if inhibited by non-specific drugs.[41] In view of this, the scientific community has been looking for selective PTP inhibitors through novel strategies to attack these enzymes, as orthosteric, allosteric, and oligomerization-inhibiting.[13] The four most potent PtpA inhibitors (compounds **5**, **9**, **18**, and **35**) were further evaluated against PtpB from *Mtb*, human PTP1B, YopH from *Yersinia enterocolitica*, human PTP-PEST, and human LYP (Table 3). In the selectivity assay, the IC_{50} of the compounds against the different phosphatases was determined. The selectivity index (SI) was represented by the IC_{50}PTP/IC_{50}PtpA ratio.

As shown in Table 3 all evaluated compounds inhibited to some extent the PTPs assessed. Among Mtb PTPs, the thiosemicarbazones

Table 3
Selectivity index (SI) values of compounds **5**, **9**, **18**, and **35** measured against some PTP representatives.[a]

Compd	5		9		18		35	
PTP	IC_{50} (μM)	SI	IC_{50} (μM)	SI	IC_{50} (μM)	SI	IC_{50} (μM)	SI
PtpA	9.5 ± 3.3	Ref value	7.4 ± 2.8	Ref value	2.9 ± 1.7	Ref value	9.1 ± 5.0	Ref value
PtpB	18.4 ± 0.9	1.9	17.6 ± 2.7	2.4	6.2 ± 1.5	2.1	30.3 ± 1.1	3.3
PTP1B	17.0 ± 3.5	1.8	> 50	> 6.8	9.4 ± 0.8	3.2	38.2 ± 8.0	4.2
YopH	7.1 ± 0.8	0.7	6.5 ± 2.3	0.9	2.6 ± 1.5	0.9	6.9 ± 1.2	0.8
PTP-PEST	> 50	> 5.3	> 50	> 6.8	15.7 ± 3.1	5.4	> 50	> 5.5
LYP	> 50	> 5.3	> 50	> 6.8	> 50	> 10.3	> 50	> 5.5

[a] Data are expressed as means ± SD of three independent experiments. The selective index (SI) is given by IC_{50}PTP/IC_{50}PtpA.

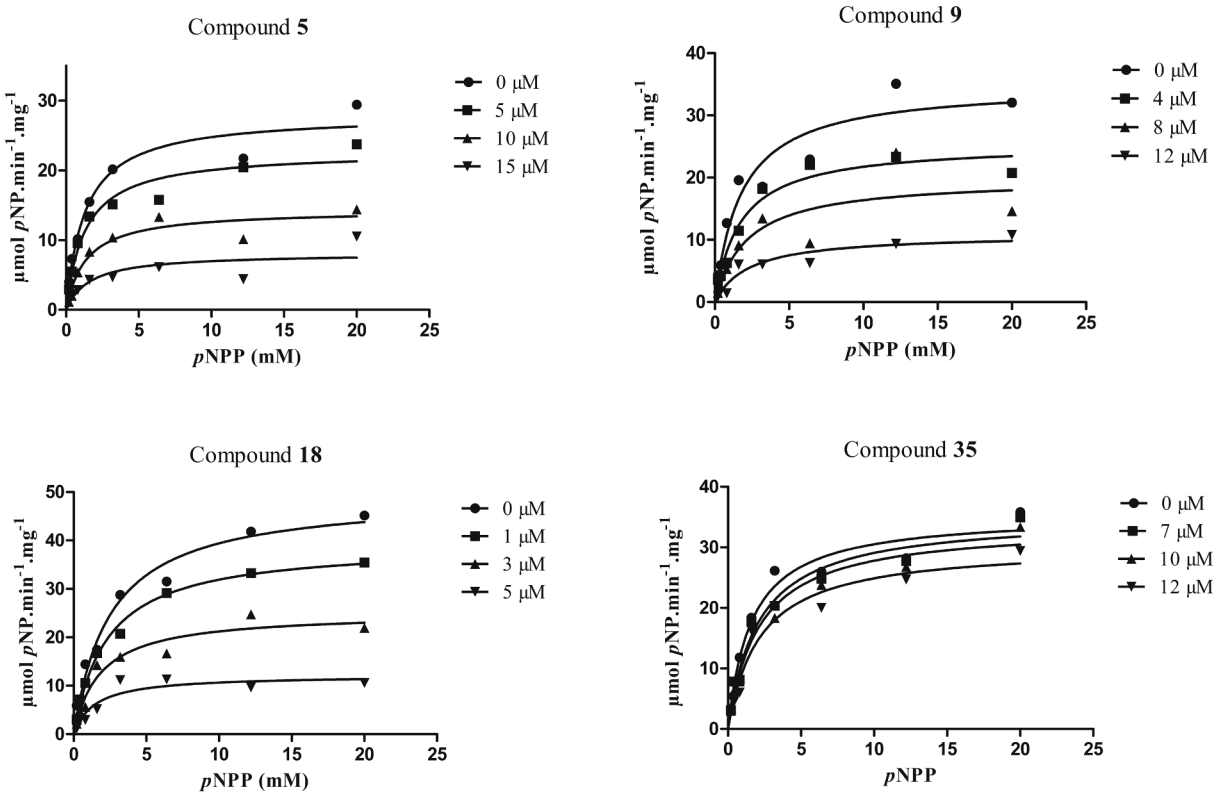

Fig. 1. Michaelis–Menten plots representing the inhibitory profile of compounds **5**, **9**, **18** and **35** against PtpA.

appear to preferentially inhibit PtpA over PtpB (SI ≥ 1.9). Regarding human PTP1B the result was similar to PtpB (SI ≥ 1.8), they preferentially inhibit PtpA, compound **9** showed the most promising specificity result over PTP1B. For human PTP-PEST and LYP, we noted the most satisfactory selectivity results, with SI values higher than 6.8. Concerning YopH, the analyzed thiosemicarbazones had an SI ≥ 0.9, indicating that they were non-selective over this enzyme. This does not represent a problem as this phosphatase is involved in diseases caused by *Yersinia* spp.[42] Compound **9** presented the most attractive results regarding its specificity for PtpA over human PTPs, among the other inhibitors highlighted (**5**, **9**, **18** and **35**), it is the only one that presents in its structure an apolar group in R_2, which might be the factor that contributes to its specificity compared to other thiosemicarbazones.

The thiosemicarbazones derivatives that were most potent against PtpA (**5**, **9**, **18** and **35**) were selected for further enzyme kinetic studies. To determine the mechanism of inhibition and K_i values, we tested three different inhibitor concentrations and seven concentrations of *p*NPP. The preliminary kinetic analysis suggested that compounds **5**, **9** and **18** presents a non-competitive mode of inhibition, on the other hand, the compound **35** showed a competitive mode of inhibition, as presented in the Michaelis–Menten plot in Fig. 1.

To the best of our knowledge, only competitive inhibitors were described for PtpA to date, therefore, this work describes the first non-competitive PtpA inhibitors. The search for inhibitors that avoid the PTPs catalytic pocket is of upmost importance, given that allosteric sites are not well conserved among PTPs, which offers a promising approach for more selective and bioavailable inhibitors.[43,44]

Analyzing the kinetic parameters, we observed that V_{max} decreases when the inhibitor concentration increased, and that K_m remains unaffected for compound **5**, **9** and **18**, suggesting a non-competitive mechanism of inhibition, with $\alpha = 1$. The kinetic parameter K_i calculated by nonlinear fit to the non-competitive inhibition equation, resulted in K_i values for thiosemicarbazones **5** of 1.2 ± 0.3 µM, for **9** of 5.6 ± 1.0 µM, and for **18** of 1.7 ± 0.3 µM for PtpA.

For the inhibitor **35**, it was observed that the V_{max} is not affected by the increase in inhibitor concentration, only the K_m values, the analysis revealed that compound **35** is a competitive inhibitor, with K_i = 12.0 ± 5.3 µM for PtpA. Accordingly, we found two different modes of inhibition of thiosemicarbazones against PtpA. Interestingly, these data indicate that the structural variation of these thiosemicarbazones significantly influences the mechanism of inhibition for this enzyme. Furthermore, all the three inhibitors (**5**, **9** and **18**) that displayed the non-competitive kinetic profile have 1-naphthyl substituent in R_1 and showed the best K_i values. The competitive inhibitor identified here, compound **35**, derived from 4-CH_3-Ph in R_1 and 5-(2-Cl,5-CF_3)-Ph-furan-2-yl in R_2 (the same substituent on compound **18** in R_2), thus the absence of the 1-naphthyl group in R_1 affected the potency and mechanism of inhibition.

To rationalize kinetics inhibition profiles, and to propose a possible binding mode of the most potent PtpA inhibitors **5**, **9**, **18**, and **35**, molecular docking simulations were carried out. A preliminary blind docking experiment (*data not shown*) revealed that compounds are able to bind within the catalytic site of *Mtb* PtpA, as well as in a site that is herein referred to as 'adjacent site' formed by residues Ala94, Arg98, Val107, Arg108, Met109, Ser112, Phe113, Pro115, His120, Leu122, Gly148, and Trp152 (see Supplementary Information Fig. S1). Notably, this site is separated from the catalytic site by the flexible D-loop (Arg111-Asp131), and was identified as a druggable site by pocket finder tools such as fpocket 1.0.[45] Accordingly, molecular docking of **5**, **9**, **18**, and **35** was performed within the catalytic site and the adjacent site described above in two independent runs.

Results of these theoretical investigations showed that PtpA inhibitors bearing a naphthyl moiety, namely **5**, **9**, and **18**, bind preferentially in the adjacent site, whereas compound **35** binds preferentially within the catalytic site, in good agreement with experimental results. This preference was defined by a combination of scores and docking poses. In detail, the naphthyl ring of **5**, **9**, and **18** was docked in a hydrophobic groove of the adjacent site in

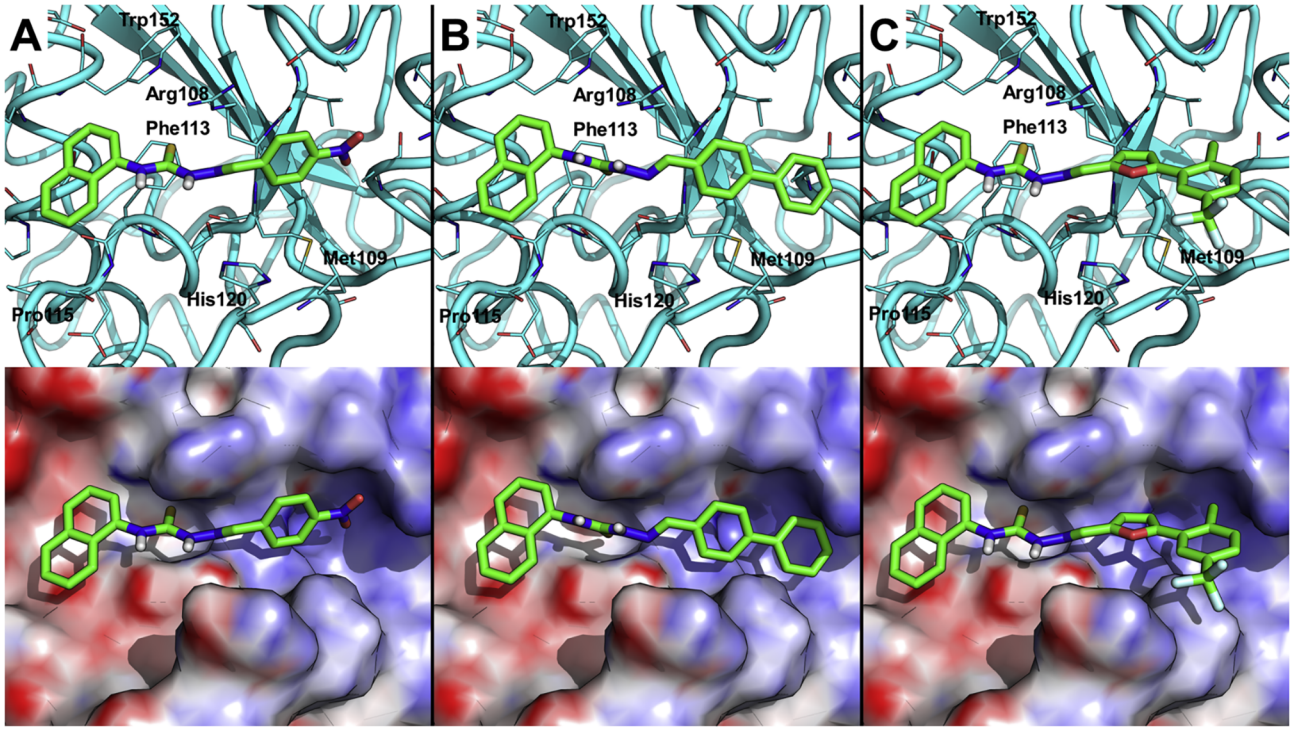

Fig. 2. Docking-based binding mode of thiosemicarbazones **5** (panel A), **9** (panel B), and **18** (panel C) within the adjacent binding site of PtpA. Compounds are showed as green sticks, the NMR solution structure of PtpA (PDB 2LUO)[46] is shown as cyan cartoon in the top panels, residues within 5 Å from the ligand are showed as lines. Residues contacted by the ligands are labeled. In the bottom panels, PtpA electrostatic surface calculated by APBS is shown. (For interpretation of the references to colour in this figure legend, the reader is referred to the web version of this article.)

Table 4
PLP score of most potent PtpA inhibitors in the two binding sites studied herein by molecular docking.

Compound	PLP score – Adjacent site	PLP score – Catalytic site
5	64.78	51.29
9	62.39	57.08
18	65.72	50.91
35	57.92	61.16

correspondence of Phe113, Pro115, Gly148, and Trp152, while the variable aromatic portion is docked in a positively charged cavity over Met109 that is delimited by Arg98, Arg108, and His120 (Fig. 2). It is worth noting that the most potent PtpA inhibitor **18** bears a phenyl ring substituted with two electron-withdrawing groups that could reinforce the binding in this particular region of the adjacent site by means of electrostatic complementarity. Notably, **35** is docked with opposed polarity in the adjacent site compared to the naphthyl derivatives, with the 2-Cl-5-CF_3-phenyl ring being docked in the hydrophobic groove (Supplementary Information Fig. S2), which may explain the lower affinity of **35** for the adjacent site compared to the catalytic site, as also highlighted by the docking scores (Table 4). Indeed, docking into the catalytic site revealed a noticeable fitting by compound **35**, which is able to bind deeper in the pocket and to mask the catalytic Cys11 residue from the solvent area (Fig. 3) with a higher docking score than **5**, **9**, and **18** (see Table 4 and Supplementary Information Fig. S3).

Overall, these theoretical results substantiate that thiosemicarbazones might bind preferentially to different binding sites of *Mtb* PtpA. Compound **35** showed a tighter binding to the catalytic site, whereas naphthyl derivatives **5**, **9**, and **18** showed a remarkable scoring preference for the adjacent site. The agreement between experimental and theoretical data reinforces the reliability of molecular modeling findings, and paves the way to further rational optimization of thiosemicarbazones as *Mtb* PtpA inhibitors.

3. Conclusions

We synthesized 49 thiosemicarbazones that were evaluated *in vitro* against recombinant PtpA from *Mtb*. Four compounds displayed reasonable inhibition, with IC_{50} lower than 9.5 μM (**5**, **9**, **18**, and **35**) and satisfactory specificity for PtpA. Our kinetic findings revealed two different inhibition mechanism for this class of molecules, interestingly, for the first-time non-competitive inhibitors for PtpA were identified, thiosemicarbazones **5**, **9** and **18** that present a naphthyl moiety at R1 showed a non-competitive mode of inhibition with a K_i of 1.2–5.6 μM. Molecular modeling highlighted the structural features important for potency and mechanism of inhibition, although all inhibitors may interact with the active site of PtpA, those with the naphthyl moiety preferably bind to an adjacent site in the structure of the enzyme. Further, this finding corroborates the modest results of selectivity found for these compounds. More importantly, our study indicates a possible allosteric binding of PtpA, some of the amino acid residues involved in the binding were in previously hot spots reported in the structure of PtpA by Silva and Tabernero.[47] Our data support that thiosemicarbazone derivatives are a novel class of potential lead compounds to further development of PtpA inhibitors and, consequently, for anti-TB drugs.

4. Experimental

All reagents were obtained commercially (Sigma-Aldrich), and all solvents used were analytical grade, without additional purification.

4.1. General procedure for the synthesis of thiosemicarbazides

Compounds **1–3** were synthesized by reacting the different isothiocyanates (10 mmol) and hydrazine hydrate (50%, 20 mmol) in 20 mL of isopropanol under magnetic stirring for 3 h at room temperature. The precipitate formed was separated by vacuum filtration and washed with isopropanol to obtain the pure product.[37]

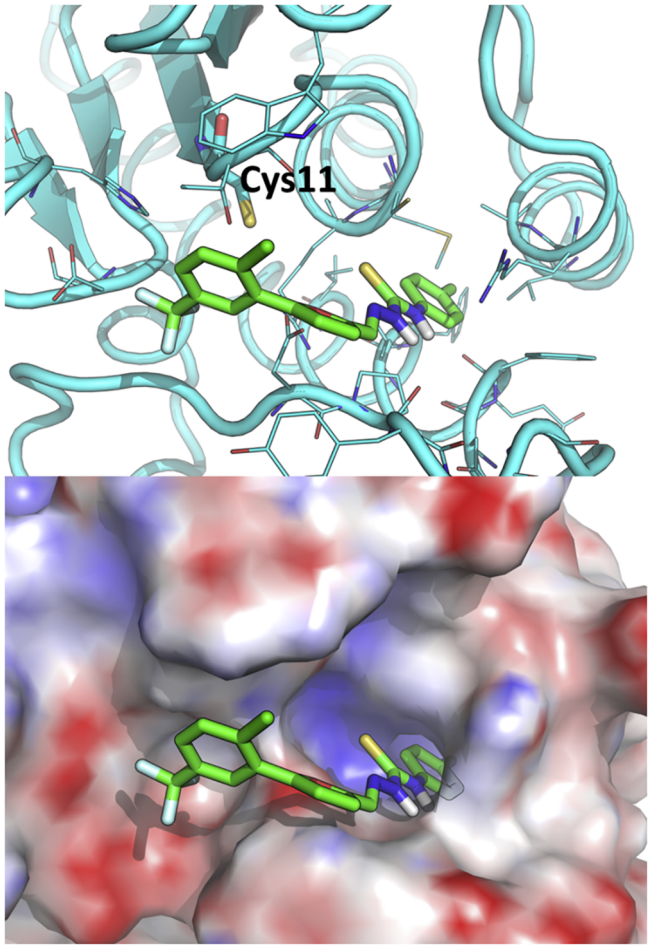

Fig. 3. Docking-based binding mode of thiosemicarbazone **35** within the catalytic site of PtpA. The compound is shown as green sticks, the NMR solution structure of PtpA (PDB 2LUO)[46] is shown as cyan cartoon in the top panel, residues within 5 Å from the ligand are showed as lines. The catalytic cysteine residue (Cys11) is shown as stick and is labeled. In the bottom panel, PtpA electrostatic surface calculated by APBS is shown (transparent surface). (For interpretation of the references to colour in this figure legend, the reader is referred to the web version of this article.)

4.2. General procedure for the synthesis of thiosemicarbazones

Thiosemicarbazones **4–52** were prepared by stirring and refluxing a solution containing thiosemicarbazide (1.19 mmol), the appropriately substituted benzaldehyde (1.25 mmol), 11 mL of ethanol, and 22 mL of water with a catalytic amount of acetic acid. After one hour, the mixture was cooled to ambient temperature, and the precipitate formed was collected by vacuum filtration and washed with water.[30]

4.3. General procedure for compound characterization

The obtained compounds were analyzed by thin-layer chromatography (TLC), using aluminum plates coated with silica gel on TLC Al foils. All synthesized compounds were characterized by ^{1}H and ^{13}C nuclear magnetic resonance (NMR) spectroscopy and melting points (mp). Melting points were determined with a Microquimica MGAPF-301 apparatus. ^{1}H and ^{13}C NMR spectra were obtained using a Bruker Ac-200F (operating at 200 MHz for ^{1}H and 50 MHz for ^{13}C) or a Bruker Avance Drx 400 spectrometer (operating at 400 MHz for ^{1}H and 100 MHz for ^{13}C), with tetramethylsilane as internal standard. The structures of all compounds were confirmed by mass spectrometry. High-resolution mass spectra (HRMS) were recorded on a micrOTOF-QII (Bruker Daltonics) mass spectrometer, equipped with an automatic syringe pump (K_D Scientific) for sample injection (constant flow of 3 μL min^{-1}), by positive mode of electron spray ionization (ESI-MS) technique (4.5 kV and 180 °C) using acetonitrile as solvent. The instrument was calibrated in the range *m/z* 50–3000 using an internal calibration standard (low concentration tuning mix solution), supplied by Agilent Technologies. Data was processed via Bruker Data Analysis software (version 4.0). When the calculated and experimental masses were compared, the error was as expected (< 2 ppm).

The synthesis and characterization compound **2** has been previously reported by the authors.[39] Data on the characterization of compounds **1** and **3** are shown below.

N-(naphthalen-1-yl)hydrazinecarbothioamide (**1**) Yield: 77%; white solid; mp 134,9–136,8 °C; ^{1}H NMR (400 MHz, DMSO-d_6) δ/ppm: 9.25 (s, 1H, N*H*), 7.96–7.94 (m, 1H), 7.90–7.88 (m, 1H), 7.81 (d, 1H, *J* 8.1 Hz), 7.67 (d, 1H, *J* 6.8 Hz), 7.54–7.49 (m, 3H). ^{13}C NMR (100 MHz, DMSO-d_6) δ/ppm: 181.7 (C═S), 135.7, 134.2, 130.2, 128.5, 126.4, 125.8, 125.2, 123.1. HRMS (ESI-TOF) *m/z*: 240.05656 $[M+H]^+$, calculated for $C_{11}H_{11}N_3S$, 240.05659.

N-(4-methoxyphenyl)hydrazinecarbothioamide (**3**) Yield: 86%; white solid; mp 138.2–139.6 °C; ^{1}H NMR (200 MHz, DMSO-d_6) δ/ppm: 8.98 (s, 1H, N*H*), 7.44 (d, 2H, *J* 8.7 Hz), 6.86 (d, 2H, *J* 8.7 Hz), 4.72 (s, 2H, NH_2), 3.73 (s, 3H). ^{13}C NMR (50 MHz, DMSO-d_6) δ/ppm: 180.4, 156.6, 132.7, 126.0, 113.7, 55.6. HRMS (ESI-TOF) *m/z*: 198.0695 $[M+H]^+$, calculated for $C_8H_{11}N_3OS$, 198.0696.

Data on the characterization of compounds **4–19** and **37–52** are shown below. The synthesis of thiosemicarbazones **20–36** was previously reported by the authors.[30]

(*E*)-2-benzylidene-*N*-(naphthalen-1-yl)hydrazinecarbothio-amide (**4**) Yield 76%; white solid; mp 217.0–218.0 °C; ^{1}H NMR (200 MHz, DMSO-d_6) δ/ppm: 11.93 (s, 1H, N*H*), 10.41 (s, 1H, N*H*), 8.22 (s,1H, -NC*H*), 8.00–7.84 (m, 5H), 7.57–7.52 (m, 4H, *J* 8.2 Hz), 7.43–7.40 (m, 3H). ^{13}C NMR (50 MHz, $CDCl_3$) δ/ppm: 177.8, 143.0, 134.3, 133.6, 133.1, 130.8, 129.7, 129.0, 128.6, 127.7, 127.5, 126.8, 126.3, 125.4, 125.2, 121.8. HRMS (ESI-TOF) *m/z*: 306.10588 $[M+H]^+$, calculated for $C_{18}H_{15}N_3S$, 306.10594.

(*E*)-*N*-(naphthalen-1-yl)-2-(4-nitrobenzylidene)hydrazine-carbothioamide (**5**) Yield 71%; yellow solid; mp 229.0–230.0 °C; ^{1}H NMR (400 MHz, DMSO-d_6) δ/ppm: 12.25 (s, 1H, N*H*), 10.66 (s, 1H, N*H*), 8.30 (s,1H), 8.24 (m, 4H), 8.01–7.98 (dd, 1H, *J* 6.0 Hz and *J* 3.0 Hz), 7.93 (d, 1H, *J* 8.5 Hz), 7.88–7.85 (dd, 1H, *J* 6,4 Hz and *J* 3,4 Hz), 7.60–7.50 (m, 4H). ^{13}C NMR (50 MHz, DMSO-d_6) δ/ppm: 178.8, 148.1, 141.2, 140.5, 136.0, 134.2, 131.0, 128.9, 128.5, 127.6, 127.0, 126.6, 126.5, 125.9, 124.2, 123.8. HRMS (ESI-TOF) *m/z*: 351.0909 $[M+H]^+$, calculated for $C_{18}H_{14}N_4O_2S$, 351.0910.

(*E*)-2-(4-chlorobenzylidene)-*N*-(naphthalen-1-yl)hydrazine- carbothioamide (**6**) Yield: 44%; white solid; mp 206.0–208.0 °C; ^{1}H NMR (200 MHz, DMSO-d_6) δ/ppm: 11.69 (s, 1H, N*H*), 10.17 (s, 1H, N*H*), 7.89 (s,1H, -NC*H*), 7.70 (d, 2H, *J* 8.3 Hz), 7.62–7.54 (m, 2H), 7.30–7.16 (m, 7H). ^{13}C NMR (50 MHz, DMSO-d_6) δ/ppm: 178.5, 141.7, 136.1, 134.8, 134.1, 133.6, 131.0, 129.7, 129.1, 128.4, 127.4, 126.9, 126.5 126.5, 125.9, 123.9. HRMS (ESI-TOF) *m/z*: 340.0674 $[M+H]^+$, calculated for $C_{18}H_{14}ClN_3S$, 340.0670.

(*E*)-2-(4-methoxybenzylidene)-*N*-(naphthalen-1-yl)hydrazine-carbothioamide (**7**) Yield: 69%; white solid; mp 203.0–205.0 °C; ^{1}H NMR (200 MHz, DMSO-d_6) δ/ppm: 11.83 (s, 1H, N*H*), 10.34 (s, 1H, N*H*), 8.16 (s,1H, -NC*H*), 8.00–7.88 (m, 5H), 7.56–7.54 (m, 4H), 6.98 (d, 2H, *J* 8.4 Hz), 3.80 (s, 3H, OCH_3). ^{13}C NMR (100 MHz, DMSO-d_6) δ/ppm: 178.0, 161.3, 143.2, 136.2, 134.2, 131.1, 129.7, 128.4, 127.3, 127.2, 126.9, 126.5, 126.4, 125.9, 123.8, 114.6, 55.8. HRMS (ESI-TOF) *m/z*: 336.1161 $[M+H]^+$, calculated for $C_{19}H_{17}N_3OS$, 336.1165.

(*E*)-2-(benzo[*d*][1,3]dioxol-5-ylmethylene)-*N*-(naphthalen-1-yl)hydrazinecarbothioamide (**8**) Yield: 60%; white solid; mp 208.0–209.0 °C; ^{1}H NMR (200 MHz, DMSO-d_6) δ/ppm: 11.84 (s, 1H, N*H*), 10.40 (s, 1H, N*H*), 8.12 (s, 1H, -NC*H*), 8.00–7.84 (m, 4H), 7.60–7.48 (m, 4H), 7.17 (d, 1H *J* 8.1 Hz), 6.95 (d, 1H, *J* 7.6 Hz), 6.06 (s, 2H).^{13}C NMR (50 MHz, DMSO-d_6) δ/ppm: 178.1, 149.4, 148.5, 142.8, 136.2, 134.1, 131.1,

129.2, 128.4, 127.3, 127.0, 126.5, 125.9, 124.7, 123.9, 108.6, 106.0, 101.9. HRMS (ESI-TOF) *m/z*: 350.0957 $[M+H]^+$, calculated for $C_{19}H_{15}N_3O_2S$, 350.0958.

(*E*)-2-([1,1′-biphenyl]-4-ylmethylene)-*N*-(naphthalen-1-yl)hy- drazinecarbothioamide (**9**) Yield: 42%; white solid; mp 204.0–206.0 °C; ^{1}H NMR (200 MHz, DMSO-d_6) δ/ppm: 11.99 (s, 1H, N*H*), 10.48 (s, 1H, N*H*), 8.26 (s, 1H, -NC*H*), 8.06–7.96 (m, 3H), 7.93–7.86 (m, 2H), 7.73 (d, 4H, *J* 7.8 Hz), 7.57–7.38 (m, 7H). ^{13}C NMR (50 MHz, DMSO-d_6) δ/ppm: 178.4, 142.8, 141.9, 139.8, 136.2, 134.2, 133.8, 131.1, 129.4, 128.7, 128.4, 128.3, 127.3, 127.3, 127.1, 126.9, 126.5, 126.4, 125.9, 123.8. HRMS (ESI-TOF) *m/z*: 382.1375 $[M+H]^+$, calculated for $C_{24}H_{19}N_3S$, 382.1372.

(*E*)-2-(4-hydroxy-3-methoxybenzylidene)-*N*-(naphthalen-1-yl)hydrazinecarbothioamide (**10**) Yield: 69%; yellow solid; mp 210.0–212.0 °C; ^{1}H NMR (400 MHz, pyridine-d_6) δ/ppm: 13.07 (s, 1H, N*H*), 11.14 (s, 1H, N*H*), 8.61 (s,1H, -NC*H*), 8.41 (d, 1H, *J* 7.9 Hz), 8.02 (d, 1H, *J* 6.8 Hz), 7.89 (d, 1H, *J* 7,9 Hz), 7.81 (m, 2H), 7.52–7.47 (m, 3H), 7.38 (d, 1H, *J* 8,1 Hz), 7.25–7.23 (m, 2H), 3.53 (s, 3H). ^{13}C NMR (50 MHz, DMSO-d_6) δ/ppm: 177.8, 149.5, 148.5, 144.0, 136.2, 134.2, 131.1, 128.4, 127.3, 126.9, 126.5, 126.4, 125.9, 125.8, 123.8, 123.2, 115.8, 110.3, 56.4. HRMS (ESI-TOF) *m/z*: 352.1112 $[M+H]^+$, calculated for $C_{19}H_{17}N_3O_2S$, 352.1114.

(*E*)-*N*-(naphthalen-1-yl)-2-(3,4,5-trimethoxybenzylidene)hy- drazinecarbothioamide (**11**) Yield: 38%; yellow solid; mp 202.0–203.0 °C; ^{1}H NMR (200 MHz, $CDCl_3$) δ/ppm: 10.75 (s, 1H, N*H*), 9.36 (s, 1H, N*H*), 8.02 (dd, 1H), 7.95 (s,1H, -NC*H*), 7.92–7.86 (m, 3H), 7.61–7.49 (m, 3H), 6.98 (s, 2H), 3.89 (s, 3H); 3.87 (s, 6H). ^{13}C NMR (50 MHz, DMSO-d_6) δ/ppm: 178.2, 153.6, 143.3, 139.7, 136.2, 134.2, 131.2, 130.0, 128.5, 127.5, 127.0, 126.6, 126.5, 125.9, 123.8, 105.4, 60.5, 56.6. HRMS (ESI-TOF) *m/z*: 396.1376 $[M+H]^+$, calculated for $C_{21}H_{21}N_3O_3S$, 396.1377.

(*E*)-*N*-(naphthalen-1-yl)-2-(naphthalen-1-ylmethylene)hydra- zinecarbothioamide (**12**) Yield: 78%; yellow solid; mp 199.0–201.0 °C; ^{1}H NMR (200 MHz, DMSO-d_6) δ/ppm: 11.98 (s, 1H, N*H*), 10.47 (s, 1H, N*H*), 9.13 (s, 1H, -NC*H*), 8.50 (d, 1H, *J* 7.2 Hz); 8.38 (d, 1H, *J* 8.0 Hz); 8.05–7.90 (m, 5H), 7.69–7.56 (m, 7H). ^{13}C NMR (50 MHz, DMSO-d_6) δ/ppm: 178.3, 141.4, 136.1, 134.2, 133.8, 131.1, 130.9, 130.8, 129.7, 129.3, 128.5, 127.6, 127.4, 126.8, 126.5, 126.0, 125.9, 123.8, 123.0. HRMS (ESI-TOF) *m/z*: 356.12160 $[M+H]^+$, calculated for $C_{22}H_{17}N_3S$, 356.12159.

(*E*)-*N*-(naphthalen-1-yl)-2-(naphthalen-2-ylmethylene)hydra- zinecarbothioamide (**13**) Yield: 63%; white solid; mp 198.0–200.0 °C; ^{1}H NMR (400 MHz, DMSO-d_6) δ/ppm: 12.07 (s, 1H, N*H*), 10.51 (s, 1H, N*H*), 8.40–8.38 (m, 2H), 8.21 (s, 1H, -NC*H*), 8.01–7.90 (m, 6H), 7.60–7.53 (m, 6H). ^{13}C NMR (100 MHz, DMSO-d_6) δ/ppm: 178.4, 143.3, 136.3, 134.2, 133.4, 132.5, 131.2, 129.6, 128.7, 128.6, 128.5, 128.2, 127.5, 127.4, 127.1, 127.0, 126.6, 126.5, 125.9, 124.0. HRMS (ESI-TOF) *m/z*: 356.1218 $[M+H]^+$, calculated for $C_{22}H_{17}N_3S$, 356.1216.

(*E*)-2-(3,4-dichlorobenzylidene)-*N*-(naphthalen-1-yl)hydra-zinecarbothioamide (**14**) Yield: 75%; white solid; mp 206.0–207.0 °C; ^{1}H NMR (200 MHz, DMSO-d_6) δ/ppm: 12.10 (s, 1H, N*H*), 10.56 (s, 1H, N*H*), 8.42 (s, 1H), 8.17 (s, 1H, -NC*H*), 8.01–7.82 (m, 4H); 7.68 (d, 1H, *J* 8.3 Hz); 7.62–7.48 (m, 4H). ^{13}C NMR (50 MHz, DMSO-d_6) δ/ppm: 178.6; 140.4; 136.1; 135.5; 134.1; 132.4; 132.2; 131.2; 131.1; 128.7; 128.4; 127.5; 127.1; 126.6; 126.5; 125.9; 123.9. HRMS (ESI-TOF) *m/z*: 374.0284 $[M+H]^+$, calculated for $C_{18}H_{13}Cl_2N_3S$, 374.0280.

(*E*)-2-(2,5-dimethoxybenzylidene)-*N*-(naphthalen-1-yl)hydra- zinecarbothioamide (**15**) Yield: 69%; white solid; mp 200.0–202.0 °C; ^{1}H NMR (200 MHz, DMSO-d_6) δ/ppm: 11.92 (s, 1H, N*H*), 10.39 (s, 1H, N*H*), 8.55 (s, 1H, -NC*H*), 7.98 (dd, 1H *J* 3.3 and 6.0 Hz), 7.91–7.84 (m,3H), 7.58–7.52 (m, 4H), 7.04–6.97 (m, 2H), 3.82 (s, 3H), 3.72 (s, 3H). ^{13}C NMR (50 MHz, DMSO-d_6) δ/ppm: 178.3, 153.8, 152.9, 138.7, 136.3, 134.1, 131.1, 128.4, 127.3, 127.0, 126.5, 125.9, 123.8, 123.3, 117.6, 113.5, 111.4, 56.7, 56.1. HRMS (ESI-TOF) *m/z*: 366.1270 $[M+H]^+$, calculated for $C_{20}H_{19}N_3O_2S$, 366.1271.

(*E*)-2-(3,4-dimethoxybenzylidene)-*N*-(naphthalen-1-yl)hydra- zinecarbothioamide (**16**) Yield: 87%; white solid; mp 217.0–218.0 °C; ^{1}H NMR (200 MHz, DMSO-d_6) δ/ppm: 11.85 (s, 1H, N*H*), 10.29 (s, 1H, N*H*), 8.15 (s,1H, -NC*H*), 7.99 (dd, 1H, *J* 6.1 Hz and *J* 2.8 Hz), 7.92–7.87 (m, 2H), 7.63–7.53 (m, 5H), 7.27 (d, 1H, *J* 7.9 Hz), 6.99 (d, 1H, *J* 7.9 Hz), 3.80 (s, 6H). ^{13}C NMR (50 MHz, DMSO-d_6) δ/ppm: 177.9, 151.2, 149.6, 143.6, 136.3, 134.1, 131.2, 128.4, 127.4, 127.2, 127.0, 126.5, 125.9, 123.9, 123.0, 111.7, 109.3, 56.2, 56.0. HRMS (ESI-TOF) *m/z*: 366.1273 $[M+H]^+$, calculated for $C_{20}H_{19}N_3O_2S$, 366,1271.

(*E*)-*N*-(naphthalen-1-yl)-2-(2-nitrobenzylidene)hydrazine-carbothioamide (**17**) Yield: 72%; yellow solid; mp 202.0–204.0 °C; ^{1}H NMR (200 MHz, DMSO-d_6) δ/ppm: 12.26 (s, 1H, N*H*), 10.56 (s, 1H, N*H*), 8.66 (s,1H, -NC*H*), 8.06 (d, 1H, *J* 8.1 Hz); 7.99 (dd, 1H, *J* 6.2 Hz and *J* 3.0 Hz); 7.92 (d, 1H, *J* 8.0 Hz); 7.88 (dd, 1H, *J* 6.3 Hz and *J* 3.0 Hz); 7.74 (dd, 1H, *J* 7.6 Hz); 7.66–7.51 (m, 6H). ^{13}C NMR (50 MHz, DMSO-d_6) δ/ppm: 178.8, 148.8, 138.1, 136.0, 134.1, 133.7, 130.9, 130.8, 129.0, 128.9, 128.4, 127.5, 126.9, 126.6, 126.5, 125.9, 125.0, 123.8. HRMS (ESI-TOF) *m/z*: 351.09101 $[M+H]^+$, calculated for $C_{18}H_{14}N_4O_2S$, 351.09102.

(*E*)-2-((5-(2-chloro-5-(trifluoromethyl)phenyl)furan-2-yl)methylene)-*N*-(naphthalen-1-yl)hydrazinecarbothioamide (**18**) Yield: 82%; yellow solid; mp 213.0–214.0 °C; ^{1}H NMR (200 MHz, DMSO-d_6) δ/ppm: 12.12 (s, 1H, N*H*), 10.32 (s, 1H, N*H*), 8.23 e 8.21 (s, s, 2H, overlapping peaks), 7.99 (dd, 1H, *J* 7.3 Hz and *J* 3.3 Hz), 7.93–7.82 (m, 3H), 7.71 (dd, 1H, *J* 1.9 Hz and *J* 8.5 Hz), 7.59–7.52 (m, 4H), 7.47 (d, 1H, *J* 3.7 Hz), 7.37 (d, 1H, *J* 7.8 Hz). ^{13}C NMR (50 MHz, DMSO-d_6) δ/ppm: 178.1; 150.9; 149.5; 135.8; 134.1; 133.6; 132.6; 132.4; 130.7; 129.2; 129.1; 128.6; 128.5; 127.3; 126.6; 126.5; 125.9; 125.8; 124.9; 124.9; 123.5; 115.3; 114.5. HRMS (ESI-TOF) *m/z*: 474.0650 $[M+H]^+$, calculated for $C_{23}H_{15}ClF_3N_3OS$, 474.0649.

(*E*)-2-(4-(dimethylamino)benzylidene)-*N*-(naphthalen-1-yl)hydrazinecarbothioamide (**19**) Yield 78%; white solid; mp 195.0–197.0 °C; ^{1}H NMR (400 MHz, DMSO-d_6) δ/ppm: 11.70 (s, 1H, N*H*), 10.22 (s, 1H, N*H*), 8.10 (s,1H, -NC*H*), 7.99–7.96 (dd, 1H, *J* 6.3 Hz and *J* 3.6 Hz), 7.90–7.86 (m, 2H), 7.73 (d, 2H, *J* 8.7 Hz), 7.57–7.52 (m, 4H), 6.72 (d, 2H, *J* 9.1 Hz), 2.97 (s, 6H). ^{13}C NMR (50 MHz, DMSO-d_6) δ/ppm: 177.4, 151.9, 144.3, 136.3, 134.2, 131.1, 129.4, 128.4, 127.2, 126.8, 126.5, 126.4, 125.9, 123.9, 121.9, 112.1, 40.2. HRMS (ESI-TOF) *m/z*: 349.1482 $[M+H]^+$, calculated for $C_{20}H_{20}N_4S$, 349.1481.

(*E*)-2-benzylidene-*N*-(4-methoxyphenyl)hydrazinecarbo-thioamide (**37**) Yield: 79%; white solid; mp 192.2–193.8 °C; ^{1}H NMR (200 MHz, $CDCl_3$) δ/ppm: 10.21 (s, 1H, N*H*), 9.05 (s, 1H, N*H*), 7.95 (s,1H, -NC*H*), 7.70–7.65 (m, 2H), 7.51–7.40 (m, 5H), 6.95 (d, 2H, *J* 8.9 Hz), 3.83 (s, 3H). ^{13}C NMR (50 MHz, $CDCl_3$) δ/ppm: 176.4, 158.1, 143.2, 133.2, 130.7, 130.6, 128.8, 127.5, 126.9, 114.1, 55.4. HRMS (ESI-TOF) *m/z*: 286.1006 $[M+H]^+$, calculated for $C_{15}H_{15}N_3OS$, 286.1009.

(*E*)-*N*-(4-methoxyphenyl)-2-(4-methylbenzylidene)hydrazine-carbothioamide (**38**) Yield: 85%; white solid; mp 174.9–175.4 °C; ^{1}H NMR (200 MHz, $CDCl_3$) δ/ppm: 10.00 (s, 1H, N*H*), 9.04 (s, 1H, N*H*), 7.90 (s,1H, -NC*H*), 7.57 (d, 2H, *J* 8.3 Hz), 7.49 (2H, *J* 8.9 Hz), 7.22 (d, 2H, *J* 8.0 Hz), 6.94 (d, 2H, *J* 8.7 Hz), 3.83 (s, 3H), 2.39 (s, 3H). ^{13}C NMR (50 MHz, $CDCl_3$) δ/ppm: 176.4, 158.0, 143.2, 141.1, 130.7, 130.4, 129.6, 127.4, 126.8, 114.0, 55.4, 21.5. HRMS (ESI-TOF) *m/z*: 300.1166 $[M+H]^+$, calculated for $C_{16}H_{17}N_3OS$, 300.1165.

(*E*)-*N*-(4-methoxyphenyl)-2-(4-nitrobenzylidene)hydrazine-carbothioamide (**39**) Yield: 44%; yellow solid; mp 200.9–202.7 °C; ^{1}H NMR (200 MHz, DMSO-d_6) δ/ppm: 12.01 (s, 1H, N*H*), 10.23 (s, 1H, N*H*), 8.27–8.21 (m,5H), 7.40 (d, 2H, *J* 8.8 Hz), 6.95 (d, 2H, *J* 9.0 Hz), 3.78 (s, 3H). ^{13}C NMR (50 MHz, DMSO-d_6) δ/ppm: 177.3, 157.6, 148.1, 141.1, 140.3, 132.2, 128.8, 128.2, 124.2, 113.8, 55.7. HRMS (ESI-TOF) *m/z*: 331.0857 $[M+H]^+$, calculated for $C_{15}H_{14}N_4O_3S$, 331.0859.

(*E*)-2-(4-chlorobenzylidene)-*N*-(4-methoxyphenyl)hydrazine-carbothioamide (**40**) Yield: 89%; white solid; mp 174.0–175.7 °C; ^{1}H NMR (200 MHz, $CDCl_3$) δ/ppm: 10.08 (s, 1H, N*H*), 9.00 (s, 1H, N*H*), 7.89 (s,1H, -NC*H*), 7.61 (d, 2H, *J* 8.7 Hz), 7.48 (2H, *J* 8.9 Hz), 7.38 (d, 2H, *J* 8.4 Hz), 6.40 (d, 2H, *J* 8.9 Hz), 3.83 (s, 3H). ^{13}C NMR (50 MHz, $CDCl_3$)

δ/ppm: 176.5, 158.1, 141.7, 136.5, 131.6, 130.5, 129.2, 128.6, 126.9, 114.1, 55.4. HRMS (ESI-TOF) *m/z*: 320.0617 $[M+H]^+$, calculated for $C_{15}H_{14}ClN_3OS$, 320.0619.

(*E*)-2-(4-methoxybenzylidene)-*N*-(4-methoxyphenyl)hydra-zine-carbothioamide (**41**) Yield: 83%; white solid; mp 159.5–161.0 °C; ^{1}H NMR (200 MHz, $CDCl_3$) δ/ppm: 10.21 (s, 1H, N*H*), 9.02 (s, 1H, N*H*), 7.91 (s,1H, -NC*H*), 7.61 (d, 2H, *J* 8.7 Hz), 7.48 (2H, *J* 8.7 Hz), 6.99–6.90 (m, 4H, overlapping peaks with *J* 8.7 Hz), 3.84 (s, 3H), 3.83 (s, 3H). ^{13}C NMR (50 MHz, $CDCl_3$) δ/ppm: 176.2, 161.7, 158.0, 142.9, 130.8, 129.1, 126.8, 125.8, 114.4, 114.0, 55.4 (2). HRMS (ESI-TOF) *m/z*: 316.1113 $[M+H]^+$, calculated for $C_{16}H_{17}N_3O_2S$, 316.1114.

(*E*)-2-(benzo[d][1,3]dioxol-5-ylmethylene)-*N*-(4-methoxy-phenyl) hydrazinecarbothioamide (**42**) Yield: 88%; white solid; mp 189.4–191.3 °C; ^{1}H NMR (200 MHz, DMSO-d_6) δ/ppm: 11.64 (s, 1H, N*H*), 10.00 (s, 1H, N*H*), 8.04 (s,1H, -NC*H*), 7.83 (s, 1H), 7.37 (d, 2H, *J* 8.9 Hz), 7.13 (d, 1H, *J* 8.3 Hz), 6.93 (m, 3H), 6.07 (s, 2H), 3.77 (s, 3H). ^{13}C NMR (50 MHz, DMSO-d_6) δ/ppm: 176.6, 157.4, 149.4, 148.5, 142.8, 132.5, 129.1, 128.1, 124.6, 113.6, 108.6, 106.0, 101.9, 55.7. HRMS (ESI-TOF) *m/z*: 330.0902 $[M+H]^+$, calculated for $C_{16}H_{15}N_3O_3S$, 330.0907.

(*E*)-2-([1,1′-biphenyl]-4-ylmethylene)-*N*-(4-methoxyphenyl)- hydrazinecarbothioamide (**43**) Yield: 97%; white solid; mp 188.1–189.3 °C; ^{1}H NMR (200 MHz, $CDCl_3$) δ/ppm: 10.23 (s, 1H, N*H*), 9.08 (s, 1H, N*H*), 7.99 (s,1H, -NC*H*), 7.75 (d, 2H, *J* 8.7 Hz); 7.66–7.60 (m, 4H); 7.53–7.38 (m, 5H); 6.95 (d, 2H, *J* 8.7 Hz); 3.83 (s, 3H). ^{13}C NMR (50 MHz, $CDCl_3$) δ/ppm: 176.5, 158.1, 143.4, 142.6, 140.0, 132.0, 130.7, 128.9, 127.9, 127.5, 127.0, 126.8, 114.1, 55.5. HRMS (ESI-TOF) *m/z*: 362.1316 $[M+H]^+$, calculated for $C_{21}H_{19}N_3OS$, 362.1322.

(*E*)-2-(4-hydroxy-3-methoxybenzylidene)-*N*-(4-methoxy-phenyl)hydrazinecarbothioamide (**44**) Yield: 86%; white solid; mp 193.1–195.0 °C; ^{1}H NMR (200 MHz, acetone-d_6) δ/ppm: 10.48 (s, 1H, N*H*), 9.64 (s, 1H, N*H*), 8.16 (s,1H, -NC*H*), 7.58–7.52 (m, 3H), 7.23 (dd, 1H, *J* 8.1 and 1.9 Hz), 6.93–6.87 (m, 3H), 3.88 (s,3H), 3.81 (s, 3H). ^{13}C NMR (50 MHz, acetone-d_6) δ/ppm: 176.7, 157.5, 149.1, 147.9, 143.1, 132.1, 126.6, 126.1, 122.5, 115.0, 113.3, 109.4, 55.6, 54.8. HRMS (ESI-TOF) *m/z*: 332.1060 $[M+H]^+$, calculated for $C_{16}H_{17}N_3O_3S$, 332.1063.

(*E*)-*N*-(4-methoxyphenyl)-2-(3,4,5-trimethoxybenzylidene)-hydrazinecarbothioamide (**45**) Yield: 86%; white solid; mp 176.3–177.5 °C; ^{1}H NMR (200 MHz, $CDCl_3$) δ/ppm: 9.92(s, 1H, N*H*), 8.96 (s, 1H, N*H*), 7.83 (s,1H, -NC*H*), 7.47 (d, 2H, *J* 8.9 Hz); 6.95 (d, 2H, *J* 8.9 Hz); 6.88 (s, 2H); 3.91 (s, 6H); 3.89 (s, 3H); 3.83 (s,3H). ^{13}C NMR (50 MHz, $CDCl_3$) δ/ppm: 176.6, 158.2, 153.6, 143.0, 140.7, 130.6, 128.3, 127.0, 114.1, 104.7, 60.9, 56.3, 55.4. HRMS (ESI-TOF) *m/z*: 376.1323 $[M+H]^+$, calculated for $C_{18}H_{21}N_3O_4S$, 376.1326.

(*E*)-*N*-(4-methoxyphenyl)-2-(naphthalen-1-ylmethylene)-hydrazinecarbothioamide (**46**) Yield: 88%; yellow solid; mp 192.8–193.5 °C; ^{1}H NMR (200 MHz, $CDCl_3$) δ/ppm: 10.16 (s, 1H, N*H*), 9.11 (s, 1H, N*H*), 8.68 (s,1H, -NC*H*), 8.40 (d, 1H, *J* 7.3 Hz), 7.98–7.89 (m, 3H), 7.63–7.49 (m, 5H), 6.94 (s, 2H, *J* 9,2 Hz), 3.83 (s, 3H). ^{13}C NMR (50 MHz, $CDCl_3$) δ/ppm: 176.5, 158.0, 141.8, 133.8, 131.2, 130.9, 130.7, 129.0, 128.7, 127.4, 126.9, 126.6, 126.3, 125.3, 123.1, 114.1, 55.4. HRMS (ESI-TOF) *m/z*: 336.1168 $[M+H]^+$, calculated for $C_{19}H_{17}N_3OS$, 336.1165.

(*E*)-*N*-(4-methoxyphenyl)-2-(naphthalen-2-ylmethylene)hy-drazinecarbothioamide (**47**) Yield: 89%; white solid; mp 204.6–206.7 °C; ^{1}H NMR (200 MHz, DMSO-d_6) δ/ppm: 11.85 (s, 1H, N*H*), 10.10 (s, 1H, N*H*), 8.34 (d, 2H, *J* 7.5 Hz); 8.17 (s,1H, -NC*H*), 8.00–7.92 (m, 3H); 7.58–7.53 (m, 2H); 7.43 (d, 2H, *J* 8.7); 6.95 (d, 2H, *J* 8.7); 3.78 (s,3H). ^{13}C NMR (50 MHz, DMSO-d_6) δ/ppm: 176.9, 157.4, 143.1, 134.2, 133.3, 132.5, 132.4, 129.5, 128.7, 128.6, 128.1, 127.5, 127.1, 123.8, 113.7, 55.7. HRMS (ESI-TOF) *m/z*: 336.1169 $[M+H]^+$, calculated for $C_{19}H_{17}N_3OS$, 336.1165.

(E)-2-(3,4-dichlorobenzylidene)-N-(4-methoxyphenyl)hydra- zine-carbothioamide (**48**) Yield: 86%; white solid; mp 185.5–186.5 °C; ^{1}H NMR (200 MHz, $CDCl_3$) δ/ppm: 10.52 (s, 1H, N*H*), 8.98 (s, 1H, N*H*), 7.89 (s,1H, -NC*H*); 7.77 (s, 1H); 7.49–7.44 (m, 4H); 6.95 (d, 2H, *J* 8.8 Hz); 3.84 (s,3H). ^{13}C NMR (50 MHz, $CDCl_3$) δ/ppm: 176.9, 158.3, 140.1, 134.6, 133.4, 133.1, 130.9, 130.4, 128.6, 126.9, 126.5, 114.1, 55.4. HRMS (ESI-TOF) *m/z*: 354.0227 $[M+H]^+$, calculated for $C_{15}H_{13}Cl_2N_3OS$, 354.0229.

(*E*)-2-(2,5-dimethoxybenzylidene)-*N*-(4-methoxyphenyl)hy-drazinecarbothioamide (**49**) Yiel 92%; white solid; mp 194.8–195.6 °C; ^{1}H NMR (200 MHz, $CDCl_3$) δ/ppm: 9.10 (s, 1H, N*H*), 9.01(s, 1H, N*H*), 8.21 (s,1H, -NC*H*), 7.50 (d, 2H, *J* 8.9 Hz), 7.38 (d, 1H, *J* 2.8 Hz),7.00–6.85 (m, 4H), 3.84, 3.83 and 3.82 (s, 9H, overlapping peaks). ^{13}C NMR (50 MHz, DMSO-d_6) δ/ppm: 176.8, 157.4, 153.8, 152.9, 138.7, 132.5, 128.2, 123.2, 117.5, 113.7, 113.5, 111.4, 56.7, 56.1, 55.7. HRMS (ESI-TOF) *m/z*: 346.1221 $[M+H]^+$, calculated for $C_{17}H_{19}N_3O_3S$, 346.1220.

(*E*)-2-(3,4-dimethoxybenzylidene)-*N*-(4-methoxyphenyl)hy-drazinecarbothioamide (**50**) Yield: 81%; yellow solid; mp 175.3–177.8 °C; ^{1}H NMR (200 MHz, $CDCl_3$) δ/ppm: 10.09 (s, 1H, N*H*), 8.98 (s, 1H, N*H*), 7.88 (s,1H, -NC*H*); 7.48 (d, 2H, *J* 8.9 Hz); 7.24 (d, 1H, *J* 2.0); 7.17 (dd, 1H, *J* 8.3 and 2.0 Hz); 6.95 (d, 2H, *J* 8.9 Hz); 6.88 (d, 1H, *J* 8.3 Hz); 3.94 and 3.93 (s, 6H); 3.83 (s, 3H). ^{13}C NMR (50 MHz, $CDCl_3$) δ/ppm: 176.3, 158.1, 151.5, 149.5, 143.4, 130.8, 127.0, 126.0, 122.4, 114.1, 111.0, 108.6, 56.1, 56.0, 55.4. HRMS (ESI-TOF) *m/z*: 346.12203 $[M+H]^+$, calculated for $C_{17}H_{19}N_3O_3S$, 346.12199.

(*E*)-*N*-(4-methoxyphenyl)-2-(2-nitrobenzylidene)hydrazine-carbothioamide (**51**) Yield: 67%; yellow solid; mp 209.3–211.6 °C; ^{1}H NMR (200 MHz, $CDCl_3$) δ/ppm: 9.45 (s, 1H, N*H*), 8.98 (s, 1H, N*H*), 8.40 (s,1H, -NC*H*); 8.06 (dd, 2H, *J* 9.2 and 7.6 Hz); 7.73–7.59 (m, 2H); 7.51 (d, 2H, *J* 8.8 Hz); 6.94 (d, 2H, *J* 8.8 Hz); 3.83 (s, 3H). ^{13}C NMR (50 MHz, DMSO-d_6) δ/ppm: 177.3, 157.5, 148.8, 137.9, 133.7, 132.2, 130.9, 129.0, 128.8, 128.0, 124.9, 113.8, 55.7. HRMS (ESI-TOF) *m/z*: 331.0863 $[M+H]^+$, calculated for $C_{15}H_{14}N_4O_3S$, 331.0859.

(*E*)-2-(4-(dimethylamino)benzylidene)-*N*-(4-methoxyphenyl) hydrazinecarbothioamide (**52**) Yield 79%; yellow solid; mp 180.1–181.8 °C; ^{1}H NMR (200 MHz, $CDCl_3$) δ/ppm: 9.89 (s, 1H, N*H*), 9.02 (s, 1H, N*H*), 7.82 (s,1H, -NC*H*), 7.52 (m, 4H overlapping peaks with *J* 8.9 Hz), 6.93 (d, 2H, *J* 8.9 Hz), 6.68 (d, 2H, *J* 8.9 Hz), 3.83 (s, 3H), 3.02 (s, 6H). ^{13}C NMR (50 MHz, $CDCl_3$) δ/ppm: 175.7, 157.8, 152.0, 144.0, 131.0, 129.0, 126.7, 120.5, 114.0, 111.7, 55.4, 40.1. HRMS (ESI-TOF) *m/z*: 329.1435 $[M+H]^+$, calculated for $C_{17}H_{20}N_4OS$, 329.1431.

4.4. PTPs expression and purification

PtpA and PtpB from *Mycobacterium tuberculosis*, YopH from *Yersinia enterocolitica,* and human PTP1B, LYP, and PTP-PEST were expressed and purified as previously described.[22,48,49]

4.5. Measurement of PtpA activity (%) and inhibition (IC50)

The phosphatase assays were carried out as previously described.[21] First, the compounds were screened in a 200 µL reaction in 96-well plates by adding 5 µL of the compounds diluted to 1 mM in dimethyl sulfoxide (100% DMSO) (final concentration of 25 µM), 20 mM imidazole pH 7.0, 50 nM PtpA (2 µL in 20 mM Tris–HCl pH 8.0, 50 mM NaCl, 5 mM EDTA, 20% glycerol, and 5 mM DTT), 10 mM *p*-nitrophenyl phosphate (*p*NPP), and Milli-Q water to complete the volume. The compound was premixed with PtpA for 10 min at 37 °C, and the reaction was started by the addition of *p*NPP. Absorbance was measured by UV–VIS spectrophotometry (TECAN Magellan Infinite M200) for 10 min at 37 °C at 410 nm with readings every 1 min. Negative controls were performed in the absence of enzyme and compound, and positive controls in the presence of enzyme and 2.5% DMSO for screening e 4% DMSO for IC_{50}. The percentage of residual activity was calculated as the difference in absorbance between times 7 min and 2 min. Compounds that reduced > 60% of the enzyme activity were selected for the IC_{50} assay. The IC_{50} was determined in the same manner as described above, but the solvent concentration was adjusted to not exceed 4% (v/v) in

the final reaction mixture and values were determined with increasing concentrations of inhibitor (0.5–50 μM) versus % of inhibition. The enzymatic activity was expressed in % of phosphatase residual activity compared with the results of wells without inhibitor. Experimental data were analyzed with GraphPad Prism 5.0 and the IC_{50} values determined by linear regression. All assays were performed in triplicate.

4.6. Selectivity assay

The selectivity assays were carried out using 2 μL of several recombinant PTPs: LYP (169 nM), PTP-PEST (205 nM), PTP1B (38 nM), and PtpB (50 nM). Assays were carried out as described above.

4.7. Enzyme kinetics

The kinetic parameters of compounds were determined by varying the concentrations of *p*NPP (0.2–20 mM) for each concentration of compound through PtpA-catalyzed hydrolysis. V_{max} and K_m were determined by fitting of the data to the Michaelis–Menten equation. Reaction rates were expressed as specific activity of the protein (μmol *p*NPP min^{-1} mg^{-1}). The kinetic parameter K_i was calculated by non-linear fits of the data to the competitive or non-competitive inhibition equation. K_i values were calculated using at least three independent experiments. Data were plotted using GraphPad Prism software.[22]

4.8. Molecular modeling

The first model of the NMR solution structure of Mtb PtpA coded by PDB ID: 2LUO was used as rigid receptor in molecular docking simulations,[46] which were carried out by the GOLD docking program.[50] The CHEMPLP scoring function was used with default parameters. Docking efficiency was increased up to 200%. While docking within the adjacent site, the binding site was centered on the side chain of Ser112 (carbon beta) and had a radius of 12 Å; while docking in the catalytic site, the binding site was centered on the catalytic cysteine Cys11 (S atom) and had a radius of 14 Å. Before molecular docking simulations, ligands were energy minimized by Szybki version 1.9.0.3 (OpenEye) at the MMFF94S force field.[51]

Acknowledgments

The authors thank the Chemistry Department of the Federal University of Santa Catarina (UFSC) and Central Laboratory of Structural Biology for providing the equipment and some of the facilities. We thank CNPq and CAPES (Brazil) for the scholarship grant and financial support.

Appendix A. Supplementary data

Supplementary data to this article can be found online at https://doi.org/10.1016/j.bmc.2018.10.030.

References

1. World Health Organization, W. 2018; Vol. 2018.
2. Souza MVND, Vasconcelos TRA. *Quim Nova.* 2005;28:678.
3. Oudghiri A, Karimi H, Chetioui F, et al. *BMC Infect Dis.* 2018;18:98.
4. Guirado E, Schlesinger LS, Kaplan G. *Semin Immunopathol.* 2013;35:563.
5. Mueller P, Pieters J. *Immunobiology.* 2006;211:549.
6. Chao J, Wong D, Zheng X, et al. *Biochim Biophys Acta (BBA) – Proteins Proteom.* 2010;1804:620.
7. Wong D, Chao JD, Av-Gay Y. *Trends Microbiol.* 2013;21:100.
8. Mascarello A, Chiaradia-Delatorre LD, Mori M, Terenzi H, Botta B. *Curr Pharm Des.* 2016;22:12.
9. Zhang Z. *ACC Chem Res.* 2017;50:122.
10. Cole ST, Brosch R, Parkhill J, et al. *Nature.* 1998;393:537.
11. Koul A, Choidas A, Treder M, et al. *J Bacteriol.* 2000;182:5425.
12. Koul A, Herget T, Klebl B, Ullrich A. *Nature Rev Microbiol.* 2004;2:189.
13. Stanford SM, Bottini N. *Trends Pharmacol Sci.* 2017;38:6.
14. Bach H, Papavinasasundaram KG, Wong D, Hmama Z, Av-Gay Y. *Cell Host Microbe.* 2008;3:316.
15. Mascarello A, Chiaradia LD, Vernal J, et al. *Bioorg Med Chem.* 2010;18:3783.
16. Manger M, Scheck M, Prinz H, et al. *ChemBioChem.* 2005;6:1749.
17. Grundner C, Perrin D, Hooft van Huijsduijnen R, et al. *Structure.* 2007;15:499.
18. Mascarello A, Mori M, Chiaradia-Delatorre LD, et al. *PLoS ONE.* 2013;8:e77081.
19. Dutta NK, He R, Pinn ML, et al. *ACS Infect Dis.* 2016;2:231.
20. Vickers C, Silva A, Chakraborty A, et al. *J Med Chem.* 2018;61(18):8337.
21. Chiaradia LD, Mascarello A, Purificação M, et al. *Bioorg Med Chem Lett.* 2008;18:6227.
22. Chiaradia LD, Martins PGA, Cordeiro MNS, et al. *J Med Chem.* 2012;55:390.
23. Oliveira KN, Chiaradia LD, Martins PGA, et al. *MedChemComm.* 2011;2:500.
24. Beraldo H. *Quim Nova.* 2004;27:461.
25. Thanh ND, Giang NTK, Quyen TH, Huong DT, Toan VN. *Eur J Med Chem.* 2016;123:532.
26. Soares MA, Lessa JA, Mendes IC, et al. *Bioorg Med Chem.* 2012;20:3396.
27. Wang Y, Gu W, Shan Y, et al. *Bioorg Med Chem.* 2017;27:2360.
28. Sebastian L, Desai A, Shampur MN, Perumal Y, Sriram D, Vasanthapuram R. *Virol J.* 2008;5:64.
29. Santacruz MCS, Fabiani M, Castro EF, Cavallaro LV, Finkielsztein LM. *Bioorg Med Chem.* 2017;25:4055.
30. de Aquino TM, Liesen AP, da Silva REA, et al. *Bioorg Med Chem.* 2008;16:446.
31. El-Sawaf AK, El-Essawy F, Nassar AA, El-Samanody EA. *J Mol Struct.* 2018;1157:381.
32. Santos FRS, Andrade JT, Sousa CSF, et al. *Med Chem.* 2018;14:1.
33. Soares MA, Almeida MA, Marins-Goulart C, Chaves OA, Echevarria A, de Oliveira MCC. *Bioorg Med Chem Lett.* 2017;27:3546.
34. Adams M, Barnard L, de Kock C, et al. *Dalton Trans.* 2016;45:5514.
35. Finch RA, Liu M-C, Grill SP, et al. *Biochem Pharmacol.* 2000;59:983.
36. Zaltariov MF, Hammerstad M, Arabshahi HJ, et al. *Inorg Chem.* 2017;56:3532.
37. Serra S, Moineaux L, Vancraeynest C, et al. *Eur J Med Chem.* 2014;82:96.
38. Lessa JA, Mendes IC, da Silva PRO, et al. *Eur J Med Chem.* 2010;45:5671.
39. Sens L, Oliveira AS, Mascarello A, Brighente IMC, Yunes RA, Nunes RJ. *J Braz Chem Soc.* 2018;29:343–352.
40. Rawls KA, Lang PT, Takeuchi J, et al. *Bioorg Med Chem Lett.* 2009;19:6851.
41. Barr A. *J Future Med Chem.* 2010;2:1563.
42. Bottini A, Wu B, Barile E, De SK, Leone M, Pellecchia M. *ChemMedChem.* 2016;11:919.
43. Krishnan N, Konidaris KF, Gasser G, Tonks NK. *J Biol Chem.* 2018;5:293.
44. Jin T, Yu H, Huang XF. *Sci Rep.* 2016;6:20766.
45. Schmidtke P, Le Guilloux V, Maupetit J, Tuffery P. *Nucleic Acids Res.* 2010;38:W582–589.
46. Stehle T, Sreeramulu S, Lohr F, et al. *J Bioogical Chem.* 2012;287:34569–34582.
47. Silva APG, Tabernero L. *Future Med Chem.* 2010;2(8):1325.
48. Siqueira JD, Menegatti ACO, Terenzi H, et al. *Polyhedron.* 2017;130:184.
49. Martins PGA, Menegatti ACO, Chiaradia-Delatorre LD, et al. *Eur J Med Chem.* 2013;64:35.
50. Verdonk ML, Cole JC, Hartshorn MJ, Murray CW, Taylor RD. *Proteins.* 2003;52:609.
51. SZYBKI 1.9.0.3: OpenEye Scientific Software, Santa Fe, NM. http://www.eyesopen.com.